Bioresource Technology 183 (2015) 221–228

Contents lists available at ScienceDirect

Bioresource Technology

journal homepage: www.elsevier.com/locate/biortech

Development and characterization of activated hydrochars from orange peels as potential adsorbents for emerging organic contaminants

M.E. Fernandez [a,b], B. Ledesma [c], S. Román [c,*], P.R. Bonelli [a,b], A.L. Cukierman [a,b,d]

[a] Programa de Investigación y Desarrollo de Fuentes Alternativas de Materias Primas y Energía (PINMATE), Departamento de Industrias, Facultad de Ciencias Exactas y Naturales, Universidad de Buenos Aires, Intendente Güiraldes 2620, Ciudad Universitaria, C1428BGA Buenos Aires, Argentina
[b] Consejo Nacional de Investigaciones Científicas y Técnicas (CONICET), Av. Rivadavia 1917, C1033AAJ Buenos Aires, Argentina
[c] Departamento de Física Aplicada, Universidad de Extremadura, Avda. Elvas s/n, 06006 Badajoz, Spain
[d] Cátedra de Farmacotecnia II, Departamento de Tecnología Farmacéutica, Facultad de Farmacia y Bioquímica, Universidad de Buenos Aires, Junín 956, C1113AAD Buenos Aires, Argentina

HIGHLIGHTS

- Orange peel-derived hydrochars are obtained by hydrothermal carbonization.
- New adsorbents are developed by thermal and chemical activation of the hydrochars.
- Adsorption of emerging contaminants depends on the adsorbents' characteristics.
- Kinetic studies are performed and adsorption isotherms are determined and modeled.

ARTICLE INFO

Article history:
Received 25 November 2014
Received in revised form 7 February 2015
Accepted 9 February 2015
Available online 17 February 2015

Keywords:
Activated hydrochars
Emerging contaminants
Hydrothermal carbonization
Orange peels

ABSTRACT

Activated hydrochars obtained from the hydrothermal carbonization of orange peels (*Citrus sinensis*) followed by various thermochemical processing were assessed as adsorbents for emerging contaminants in water. Thermal activation under flows of CO_2 or air as well as chemical activation with phosphoric acid were applied to the hydrochars. Their characteristics were analyzed and related to their ability to uptake three pharmaceuticals (diclofenac sodium, salicylic acid and flurbiprofen) considered as emerging contaminants. The hydrothermal carbonization and subsequent activations promoted substantial chemical transformations which affected the surface properties of the activated hydrochars; they exhibited specific surface areas ranging from 300 to ~620 m^2/g. Morphological characterization showed the development of coral-like microspheres dominating the surface of most hydrochars. Their ability to adsorb the three pharmaceuticals selected was found largely dependent on whether the molecules were ionized or in their neutral form and on the porosity developed by the new adsorbents.

1. Introduction

Hydrothermal carbonization (HTC) of biomassic residues has been recently revived and employed as a way to obtain a solid product with higher carbon content than the original material. The HTC of a biomass is achieved using water as the reaction medium and applying mild temperatures (180–250 °C) under saturated pressure (autogenous or provided by a gas) for several hours. The thermochemical process applied to biomass includes simultaneous reactions of hydrolysis, dehydration, decarboxylation, condensation, polymerization and aromatization of the original precursor, although detailed reaction mechanisms are yet unknown due to the complexity of this type of natural materials (Funke and Ziegler, 2010). The resulting carbon-rich product, known as hydrochar, usually exhibits increased heating values when compared to the natural biomass (Román et al., 2012), showing potentiality as an energy source; moreover, functional groups on its surface have been identified, which may improve their chemical reactivity and potentialities towards certain applications such as adsorption (Román et al., 2013).

In this regard, available agro-industrial residues have been investigated as precursor of hydrochars. They include materials as diverse as sunflower stems, walnut shells and olive stones (Román et al., 2012), poultry manure and corn silage (Oliveira et al., 2013), and palm empty fruit bunches (Parshetti et al.,

* Corresponding author. Tel.: +34 924289600; fax: +34 924289601.
E-mail address: sroman@unex.es (S. Román).

http://dx.doi.org/10.1016/j.biortech.2015.02.035
0960-8524/

2013), among others. In particular, orange peels discarded from juice processing industry are a valuable waste material ubiquitously available. Global orange production for 2013/14 is currently estimated at 51.8 million metric tons, with a substantial fraction destined to industrialization (FAS-USDA, 2014). These peels represent a significant disposal problem, especially in those regions where orange cultivation is a major industry (Fernandez et al., 2014). As far as the authors know, their conversion into hydrochars has only been reported by Titirici et al. (2007) who compared mechanical soft and hard biomass as precursors.

Most of the hydrochars developed have been investigated as a mean to upgrade biomass feedstock quality for energy generation (Parshetti et al., 2013; Román et al., 2012), for CO_2 storage (Hao et al., 2013) or for soil amendment (Oliveira et al., 2013). However, recently, hydrochars have also been regarded as potential carbonaceous adsorbents. In general, carbonaceous adsorbents can be defined as materials mainly composed of carbon, which have porosity and/or surface chemistry characteristics suitable to enhance the adhesion of molecules to their surface. Several carbon adsorbents have been developed so far. In particular, activated carbons (ACs) still stand out mainly due to their ease of preparation, which does not require very sophisticated experimental set-up in comparison with other methods and the possibility of using heterogeneous sources such as biomass as starting materials. This also allows giving an added value to agro-industrial wastes. ACs are usually produced by physical or chemical activation. Both processes require a pyrolysis stage either prior or after the reaction with the gasifying or oxidizing agent (Rodriguez Reinoso, 2002). Usually the pyrolytic stage involves the use of high temperatures (above 600 °C) as well as the use of high purity inert gases. In this frame, the possibility of performing the carbonization step via HTC instead of pyrolysis can result in important energy and economical cost reduction, apart from other handling advantages derived from the greater simplicity of the process (such as tar formation, which is an important issue specially with materials with high content of volatile matter, such as biomass). Because of these advantages, the possibility of activating hydrochars has recently become a hot topic for research (Román et al., 2013; Hao et al., 2013).

On the other hand, the effect of adding chemicals during the HTC of biomass and pure carbohydrates has been examined before, regarding the control of pH during the process by addition of citric acid (Titirici et al., 2007). Also, the effect of acetic acid and lithium chloride on the energy and mass yields and on the constituents of the original biomass (Lynam et al., 2011) or the use of KOH for the activation of glucose-derived carbon spheres with potential as functional materials (Li et al., 2011) have been investigated. However, adding chemicals to tailor the surface chemistry of a biomass-derived hydrochar and to provide a specific functionalization or to improve its textural characteristics has been scarcely studied (Falco et al., 2013; Hao et al., 2013). Despite the number of pieces of research on the improvement of chemical or structural properties of hydrochars has increased during last years, there is still a gap on the use of novel precursors which had been traditionally discarded for classical activation methods, such as biomass with high humidity content. To the best of the authors' knowledge, no studies dealing with the activation of hydrochar obtained from orange peels and their potential use as adsorbents have been reported.

As it is well-known, the versatility of carbonaceous adsorbents like ACs makes them suitable to be used in a large variety of systems such as drinking water and wastewater treatments, and applications in the food, beverage and chemical industries. The literature offers a wide spectrum of studies on their use to remove a large variety of organic molecules with different toxicity, abundance, polarity or size characteristics, including phenolic compounds (in the form of phenol or its derivatives, such as nitrophenol, aminophenol or chlorophenol), volatile organic compounds (benzene, toluene or n-hexane) and synthetic dyes (methylene blue, methyl orange or acid green), to name a few (Bansal and Goyal, 2001; Fernandez et al., 2014). Lately, the organic compounds categorized as emerging have driven some attention. They include pharmaceuticals, steroid hormones, pesticides, personal care products and other industrial chemicals in very low concentrations (ng/L to μg/L). Discharge guidelines and standards do not exist for most of them and their removal within wastewater treatment facilities is commonly variable and incomplete (Luo et al., 2014). Although their environmental significance and fate remain poorly understood, their presence has been associated to toxic and ecological effects on biota (Delgado et al., 2012). With respect to adsorption of emerging contaminants onto ACs, many publications have given evidence about the suitability of these adsorbents for removal of herbicides and pesticides, drugs, and personal care products (Delgado et al., 2012). However, few attempts have been made to test activated hydrochars for contaminants removal from water such as atrazine and tetracycline.

With these premises, the present study is devoted to investigate the feasibility of obtaining adsorbents through the conversion of orange peels into hydrochars by means of HTC and their further processing by thermal and chemical activation. The resulting activated hydrochars are characterized and comparatively analyzed, and their behavior in the adsorption of three emerging pharmaceutical contaminants is examined. Particularly, two non-steroidal anti-inflammatory drugs: diclofenac sodium (DFS), frequently detected in wastewaters, and flurbiprofen (FP), of more recent occurrence (Verlicchi et al., 2012) were selected; also, salicylic acid (SA), an aspirin metabolite frequently found in municipal and industrial discharges, was investigated (Luo et al., 2014). To the authors' knowledge, the removal of these compounds has not been studied before onto hydrochar-based ACs.

2. Methods

2.1. Materials

Oranges (*Citrus sinensis*) from southeastern Spain, were purchased from a local market, washed and peeled. The orange peels were chopped and oven-dried at 100 °C. The dried samples were then crushed, milled and screen-sieved (0.5–1 mm). The precursor material obtained is hereafter abbreviated as OPP.

Pharmacopoeia grade SA (M.W. 194.2 g/mol, Standard®), FP (M.W. 244.3 g/mol, Gador®), DFS (M.W. 318.1 g/mol, Henan Dongtai Pharm Co. Ltd.) and analytical grade H_3PO_4 acid (Biopack®) were employed.

2.2. Hydrochar production

A mass of 10 g of OPP was soaked with 100 mL of distilled water and allowed to hydrate for 2 h within a Teflon vessel. The HTC of the precursor was carried out in a stainless steel autoclave (Berghof, Germany), heated at 200 °C for 20 h under self-generated pressure conditions. These experimental conditions were chosen based on previous works with agricultural residues (Román et al., 2012; Titirici et al., 2007). Then, the sample was rapidly cooled to room temperature immersing the reactor in an ice bath, and the solid was collected by filtration and sequentially washed with warm distilled water and finally dried at 100 °C. The hydrochar obtained is hereafter abbreviated as HC.

2.3. Hydrochar activations

Thermal activation of the HC (4 g) was performed inside a cylindrical stainless steel atmospheric pressure reactor described

elsewhere (Gañán et al., 2006) under a steady flow of CO_2 (40 mL/min) at 750 °C, or air (70 mL/min) at 300 °C; the time was set at 1.5 h. The choice of these conditions was based on previous experiments with OPP. The two activated hydrochars obtained are hereafter labeled as HC-C and HC-A, respectively. It is worthwhile to mention that OPP showed greater reactivity towards thermal activation than other biomass materials previously tested in the same experimental installation (Román et al., 2013). Therefore, the selected conditions used in this study were milder than those employed for other biomass-based HCs.

Chemical activation was performed following a procedure similar to that reported by Hao et al. (2013). Briefly, 2 g of HC were contacted with a 50% phosphoric acid solution, in a 4:1 acid/precursor weight ratio, kept overnight at room temperature, and then dried at 100 °C for 2 h. The dried impregnated sample (HC-P) was then activated under a flow of N_2 (70 mL/min) at 600 °C, held for 1 h. Finally, the activated hydrochar was exhaustively washed with distilled water. It is hereafter abbreviated as HC-PN. Also, another acid hydrochar (AHC) was developed contacting 10 g of OPP with 100 mL of a 50% phosphoric acid solution and left to stand for 2 h within the Teflon vessel. The rest of the procedure was analogous to that for the production of HC earlier described. A sample of AHC (2 g) was also activated under a flow of N_2, in the same conditions as for HC-PN. This activated hydrochar is abbreviated as AHC-N. A schematic representation of the different activation procedures employed, along with the acronyms used for the resulting products, is illustrated in Fig. S1.

2.4. Characterization

Elemental composition of the samples was assessed by means of an automatic elemental analyzer (Carlo Erba model EA 1108). Their surface chemistry was studied through the determination of the point of zero charge (p_{zc}). It was estimated from the pH of a concentrated dispersion, following the procedure given in detail elsewhere (Carrott et al., 2001). Identification of surface functionalities was complementarily conducted by Fourier Transformed infrared (FT-IR) spectroscopy. The spectra were recorded by transmission method (Perkin-Elmer IR Spectrum BXII spectrometer) within the wavenumber range 600–4000 cm^{-1}.

Scanning electron microscopy (SEM) was performed in a Zeiss Supra 40 microscope equipped with a field emission gun. The images were taken with an in-lens detector and acceleration voltage was set at 3 kV. The samples were placed on an aluminum holder, supported on conductive carbon tape and sputter coated with Pt.

Textural properties were assessed from N_2 adsorption isotherms at −196 °C (AUTOSORB-1, Quantachrome), according to conventional procedures (Fernandez et al., 2014). The Brunauer–Emmett–Teller (BET) surface area (S_{BET}) was determined by the standard BET procedure; total pore volume (V_t) was estimated from the amount of nitrogen adsorbed at the relative pressure of 0.95, and the mean pore width (W) was calculated from $W = 4\ V_t/S_{BET}$. The external surface (S_{ext}) was assessed by the α-method, using a reference non-porous solid, as described in previous works (Román et al., 2013), the volume of micropores was determined through the Dubinin–Radushkevich equation (V_{miDR}), and the volume of mesopores (V_{me}) was estimated as the difference between V_t and V_{miDR}.

2.5. Batch adsorption studies

In order to assess the potentiality of the materials obtained for contaminants removal, batch adsorption experiments were performed in glass flasks within a batch thermostatized system at 25 ± 1 °C, under a wrist-action shaker agitation at 500 rpm. The stability of DFS, FP and SA solutions at different pHs was previously investigated. The adsorption performance of all adsorbents with the three drugs was tested comparatively at neutral pH and, taking into account the p*K*a of the adsorbates, it was also investigated at acid pH (pH = 2) in the case of SA and FP; this condition was not studied for DFS, because this drug is inactivated under acidic conditions (Jodeh et al., 2015). The solution's pH was maintained with the aid of a buffer phosphate and HCl, respectively.

From these previous experiments, the pH that led to the best adsorption performance was selected and kinetic studies were performed contacting 0.015 g of each activated hydrochar with 30 mL of 0.05 mM DFS, FP or SA solutions, indistinctly. Samples were withdrawn at appropriate time intervals, the slurries were filtered through 0.45 μm membranes and concentrations of DFS, FP and SA in solution were obtained from the measured absorbance in the supernatant at their λ_{max} (275, 247 and 297 nm, respectively) by means of an UV–Vis spectrophotometer (Shimadzu Model UV mini 1240). Equilibrium adsorption isotherms were also obtained by contacting 0.015 g of each activated hydrochar with 30 mL of each drug solutions of different initial concentrations (0.05–2 mmol/L) until equilibrium was attained. Tests were carried out at least in duplicate. Average values are reported.

3. Results and discussion

3.1. Characterization

The overall solid yields (defined as the percentage of the original precursor weight that remains after HTC and further activation treatments) are presented in Table 1. The yield value obtained for HC was very similar to those obtained from other lignocellulosic precursors (Román et al., 2012) and the same as that obtained from orange peels by Titirici et al. (2007). The brown color of the hydrochars implied a partial carbonized product. The yield value obtained for AHC was very similar to HC, indicating that the acid addition had almost no pronounced effect. This result is in agreement with that reported by Lu et al. (2014) who only found significant differences in the solid yields at very early stages of the HTC of cellulose (with either HCl or H_2SO_4), while further prolongation of the process had no effect on these yields. The activation of HC with CO_2 (HC-C) changed significantly its aspect and reduced the yield of the product obtained due to the loss of a great amount of volatile compounds and partial CO_2 gasification. Among all samples, the lowest solid yield was attained for the air activated sample (HC-A) owing to the significant burn-off. Overall solid yields for HC-PN and AHC-N were slightly higher than for the rest of the activated hydrochars, presumably because phosphoric acid may have promoted crosslinking reactions that could help to retain some low molecular weight species into the solid phase (Vernersson et al., 2002).

Table 1
Overall solid yields, elemental composition and point of zero charge (p_{zc}) for the precursor, the hydrochars and the activated hydrochars.

Sample	Overall solid yield [%]	Elemental composition [w%][a]				p_{zc}
		C	H	N	O[b]	
OPP	–	44.1	5.8	0.8	49.3	–
HC	37.0	65.8	5.1	0.5	28.6	6.0
HC-C	17.3	83.9	1.4	0.4	14.3	10.3
HC-A	11.6	67.0	1.7	1.3	30.0	4.9
HC-PN	23.5	73.1	1.3	0.3	25.3	2.8
AHC	38.4	67.7	4.2	0.0	28.1	6.2
AHC-N	19.8	84.2	1.2	0.1	14.5	5.3

[a] Dry and ash-free basis.
[b] Estimated by difference.

The elemental composition of the solids changed significantly as a consequence of the hydrothermal carbonization and activation processes. The results obtained are also presented in Table 1. Both HC and AHC showed similar values, suggesting that during the HTC the presence of the acid did not alter significantly the solid obtained. The increase in the carbon content of both hydrochars suggests that a substantial fraction of the carbon in OPP was stored in these solids, while hydrogen and oxygen decrease is consistent with the removal of volatile compounds during the HTC. At the temperature applied (200 °C), the decomposition of hemicelluloses and pectins has been reported by other authors (Lynam et al., 2011; White et al., 2010). Activation of the hydrochars resulted in a further increase in C content and a decrease in the rest of the elements for HC-C. As expected, air-activated hydrochar showed some increase in oxygen content in comparison to HC. Chemically activated samples exhibited the lowest N content. HC-PN showed only a small increase in the C content and, conversely, AHC-N displayed an elemental composition comparable to that of CO_2-activated hydrochar. Neither the precursor nor the hydrochars contained sulfur which is ecological and technologically favorable.

Additionally, the variation in the elemental composition of the samples was analyzed based on the H/C and O/C atomic ratios, via the Van Krevelen diagram that accounts for the demethanation, dehydration and decarboxylation of the samples that take place during the carbonization process (Parshetti et al., 2013). The diagram is illustrated in Fig. 1. In general, both H/C and O/C ratios decreased sharply with increasing temperature of the treatments. Dehydration of the biomass is one of the main mechanisms for the removal of O and H from hydrochars, which also improves its fuel value (Lynam et al., 2011). A high concentration of oxygen in the air-activated sample may indicate that there were still many oxygen-containing groups besides the carboxylic ones. Activation of the hydrochars may also be related to the release of methane, suggesting the cleavage of aliphatic side chains and leading to the augmentation of aromaticity of the carbonaceous structures (Jagtoyen and Derbyshire, 1998). Furthermore, the decrease in O/C ratio might have also turned the surface less hydrophilic (Chen and Chen, 2009).

The selection of activation conditions allows the tailoring of the adsorbent's surface chemistry towards a material with predominance of basic or acidic functional groups in benefit of the selective uptake of contaminants with shared characteristics. This is well represented by the values of p_{zc} obtained for the hydrochars and activated hydrochars, which are displayed in Table 1. Again, the similarity of HC and AHC is reinforced by equivalent values of the p_{zc}. Clearly, the hydrochar activated with CO_2 (HC-C) developed a strong basic character whereas those activated with air (HC-A) or phosphoric acid (HC-PN and AHC-N) exhibited an acidic character, which may derive from a greater abundance of oxygenated functional groups on their surface.

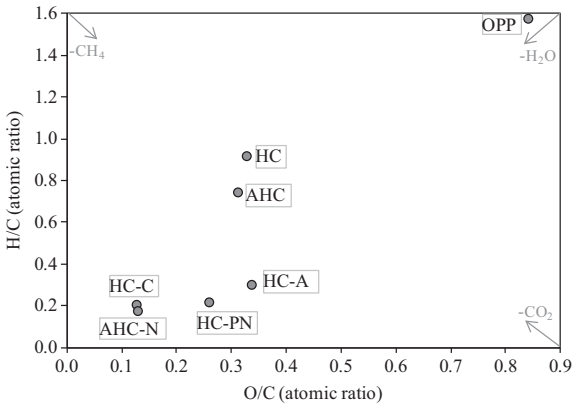

Fig. 1. Van Krevelen diagram for the precursor, the hydrochars and the activated hydrochars.

Further insight into possible functional groups present on the surface of the samples was obtained from their FT-IR spectra (Fig. S2). Fig. S2a shows the spectra for the heterogeneous precursor and the hydrochars obtained. As may be observed, the HTC of the precursor at 200 °C resulted in the loss of polysaccharide character, evidenced by the diminished intensity of peaks in the regions 1160–1000 cm^{-1} and at 1780–1580 cm^{-1} relative to carboxylic and carboxylate groups observed in HC. A reduced intensity of the carbonyl band (1615 cm^{-1}) and an associated band shift to lower wavenumbers from 1734 cm^{-1} (OPP) to 1700 cm^{-1} (HC) are observed, as other C—O containing functionalities (olefinic, vinyl ethers and lactones) may appear during the polysaccharide decomposition (White et al., 2010). The broad absorption peak around 3420 cm^{-1}, related to H-bonded hydroxyl groups from carboxyls, phenols and chemisorbed water, was also highly reduced in HC, possibly due to the dehydration process undergone during the hydrothermal carbonization. However, the presence of this band together with another small one around 1060 cm^{-1} may indicate that HC remained with a significant number of —OH groups on its surface (Li et al., 2011). The spectra for the thermally and chemically activated hydrochars is illustrated in Fig. S2b. Activation of hydrochars seemed to further decrease the amount of functional groups. The peak at 2920 cm^{-1} (stretching vibrations of aliphatic C—H bonds) almost disappeared with thermal activation. For HC-A, the absence of peaks at 2920 and 1700 cm^{-1} suggests lower content of aliphatic substituents within the aromatic structures of the activated hydrochar and the decomposition of the carboxylic groups at relatively low temperature. Moreover, the peak at 1437 cm^{-1}, assigned to symmetrical vibration of ionic carboxyl groups also disappeared in HC-A (Schiewer and Iqbal, 2010). The peak at 1615 cm^{-1} assigned to carboxylate groups and C=C bonds in aromatic compounds was slightly more prominent compared to that in HC spectrum, which could be due to an increase in aromaticity and on the amount of oxygen in the former sample (Román et al., 2013). The lack of peaks in HC-C would be the result of the decomposition and cracking of a great number of carbohydrate structures originally present in OPP. Two small widen peaks are observed around 1520 and 1140 cm^{-1} denoting the existence of aromatic structures. While in HC and AHC spectra both peaks at 1617 and 1700 cm^{-1} were still present, HC-PN and AHC-N spectra only displayed a single peak at 1612 cm^{-1} that accounts for the complete disappearance of carboxylic groups and the presence of aromatic C=C and C=O, indicating that only hard carbon components remained (Chen and Chen, 2009). Also, AHC presented a slight peak at 1274 cm^{-1} associated to free P—O bonds while HC-PN showed a peak shifted to 1225 cm^{-1} that may be assigned to P—O—C bonds in aryl structures, suggesting the incorporation of phosphate and polyphosphate groups to the solid. The distinct structures and surface characteristics of the hydrochars obtained from the orange peels, arising from the different treatments applied, would significantly impact on their affinity towards contaminant molecules.

Fig. 2a and b display the N_2 adsorption isotherms for all the samples, while textural parameters, as evaluated from these isotherms, are reported in Table 2. As can be observed, OPP showed negligible BET surface area and total pore volume, in agreement with results reported by other authors (Fernandez et al., 2014; Thirumavalavan et al., 2011). The HTC of OPP promoted a slight development of porosity. A rather low S_{BET} was obtained for HC likely due to incomplete carbonization and the permanence of disorganized matter within the porous structure. Low S_{BET} have also been reported for hydrochars obtained from other agricultural

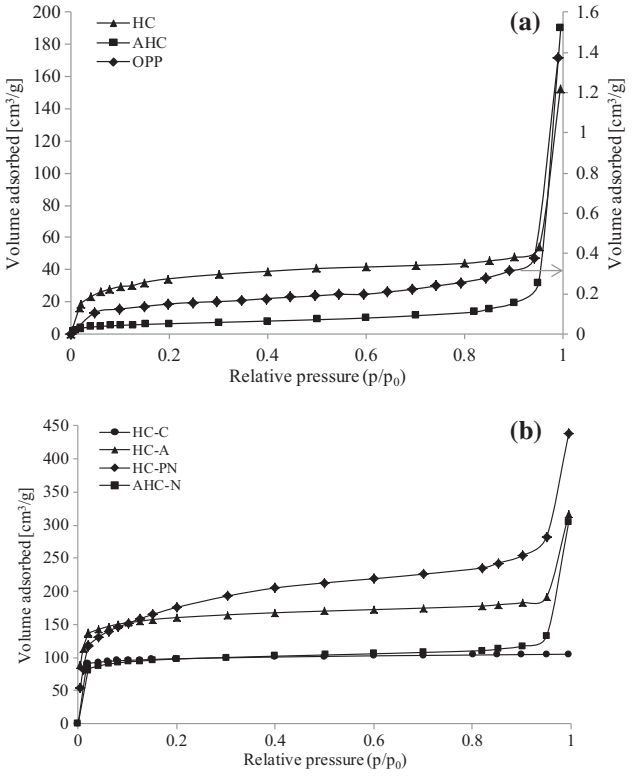

Fig. 2. N_2 adsorption isotherms onto (a) the precursor and the hydrochars, and (b) the activated hydrochars.

wastes (Román et al., 2013; Titirici et al., 2007). The isotherm obtained for HC featured an intermediate between type I and II of the IUPAC classification, a combination of microporous–mesoporous structures. AHC presented even a lower S_{BET} than HC, possibly as a result of the hydrolysis of some cellular components of the hydrochars by the effect of the H_3PO_4 acid and the partial blockage of the pores. A large increase in N_2 adsorption was observed at $p/p_0 > 0.9$, suggesting that the surface area measured matched the external surface area in AHC (Sevilla et al., 2011), as evidenced by the values displayed in Table 2.

Regardless of the activating conditions, all the activated hydrochars exhibited a greater development of porosity and specific surface area, as compared to the parent hydrochar. As found in most of the studies dealing with HCs, the porosity development of HC is very scant (Sevilla et al., 2011; Román et al., 2012), due to the permanence of decomposition products on the HC surface and, additionally, the highly acid hydrochar surface, which tends to chemisorb oxygen from air, thus causing porosity blockage (Román et al., 2012). Activation brings about the selective removal of C atoms from the hydrochars surface and in consequence the pore volume is increased. Moreover, there are some differences

Table 2
Textural characteristics of the precursor, the hydrochars and the activated hydrochars.

Material	S_{BET} [m^2/g]	S_{ext} [m^2/g]	V_{miDR} [cm^3/g]	V_{me} [cm^3/g]	W [nm]
OPP	0.4	0.2	0.0003	0.0002	5.0
HC	117	18	0.059	0.025	2.7
HC-C	301	10	0.154	0.008	2.1
HC-A	499	35	0.255	0.025	2.2
HC-PN	618	104	0.291	0.102	2.8
AHC	23	23	0.011	0.019	5.2
AHC-N	304	31	0.156	0.024	2.4

on the way the different activating agents react with the carbon, and this in turn affects the surface features of the final adsorbent. For example, HC-A developed common characteristics of a microporous material, with a slight contribution of mesoporosity, and a relatively large S_{BET}, in coherence with previous works dealing with air activated carbons (Rodriguez Reinoso, 2002). On the other hand, even when activation with CO_2 did not provoke an important increase in its S_{BET}, it can be seen that the isotherm obtained for HC-C was the only one that displayed exclusively type I characteristics, indicating the development of an essentially microporous structure. This result is consistent with the CO_2 acting way, which primarily reacts with the active sites located in the centers of the pores, thus creating microporosity, and only when large periods of time are used, it reacts with the active sites located in the pore walls, widening the porosity (Rodriguez Reinoso, 2002).

With respect to the chemically activated hydrochars, HC-PN presented a noticeable higher specific surface area and pore volume in comparison to those samples thermally activated with either CO_2 or air; this agrees with the results obtained by Hao et al. (2013). The H_3PO_4 acid may have reacted with HC structural compounds and induced further depolymerization, provoking a global pore volume development. Conversely, because AHC was washed after HTC step, the amount of acid impregnating the sample when the activation step was carried out was sensibly lower in comparison to HC impregnated with the acid. This may have been related to the inferior development of porosity obtained for AHC-N.

The SEM micrographs of the samples were obtained and are supplied as Supplementary data. Firstly, a very clear difference in the surface of the original OPP and the resulting hydrochar may be observed from the comparison of Fig. S3a and b, respectively. While OPP presented flattened thin walls with clean and undulated surfaces, some fully developed spheres but mostly partially developed ones, in coral-like shapes, covered the surface of HC after the HTC of the orange peels. The formation of these microparticles of different sizes and shapes has been attributed to the decomposition of cellulosic components and the recombination of the cellulose fragments, which have been associated to HTC temperatures above 190 °C (Sevilla et al., 2011). The adoption of a spherical form is related to the microparticles hydrophobicity, as this shape minimizes their contacting interface with the surrounding water (Falco et al., 2013). However, in this case, most of the particles appeared fused to one another. Li et al. (2011) observed that prolonged times of HTC can cause the fusion of the microspheres into particles with peanut-like and other irregular shapes. The fused microparticles could remain anchored to the surface of the hydrochar which maintained some of the structural scaffold of OPP, most likely as a consequence of the chemical stability of some of the constituents of the peel that are only partially degraded (Sevilla et al., 2011).

Fig. S3c and d illustrate the effect of the thermal activation on the surface morphology of the hydrochar developed. CO_2 activation of the hydrochar provoked a more extended fusion of the microspheres, creating spheroidal particles with sizes over 2 μm (Figure not shown) as a result of the coalescence of smaller spheres into larger ones; however, as shown in Fig. S3c, the coral-like shapes observed in the original hydrochar remained. HC-C possessed not only larger fused microparticles but also smoother than those observed in the air-activated hydrochar (Fig. S3d). HC-A had well developed spheroidal particles with the smallest distribution of sizes, up to 100 nm diameter; also, rough surfaces with very small cavities were observed. The decrease in the mean diameter may have been caused by their loosely crossed-linked outer structure (Li et al., 2011). In agreement with the results of Román et al. (2013), the hydrochar activated with air presented a more extended development of these particles than that activated with CO_2. The enhanced fusion of microspheres as a consequence of greater temperatures for CO_2 activation may also be suggested.

The effect of the phosphoric acid on the hydrochar impregnated and further activated is depicted in Fig. S3e and on the hydrochar developed with the acid and then activated in Fig. S3f and g, respectively. Chemical activation promoted the growth of more spherical particles. The SEM image of HC-PN (Fig. S3e) shows that the resulting particles had a more spherical shape after the thermal treatment of HC impregnated with the acid whose surface appeared to be fused and similar to that of the original HC (Fig. S3b). Moreover, the particles' surface was rough and covered with spikes. Unlike HC, AHC presented smaller spherical particles, less fused to one another, but still attached to the walls' surface of the material, likely as a result of highly reactive fragments forming precipitates by condensation reactions (Funke and Ziegler, 2010). AHC-N showed clusters of partially developed spheres in coral-like shapes but with smooth surfaces. This suggests that the roughness of the particles obtained may be linked to the presence of the acid.

3.2. Adsorption studies

The performance of the activated hydrochars as potential adsorbents of emerging contaminants was investigated. As a consequence of the partial carbonization of the hydrochars, some colored compounds were released to the aqueous solutions during the experiments. Suitable adsorbents were obtained only through further modification of the hydrochars and, therefore, only the samples subjected to activation were tested. For adsorption studies with DFS, as mentioned before, solutions at acidic pH were not used. At a solution pH lower than its p*K*a (p*K*a = 4.2), this drug would be mainly in its neutral form and may undergo an intramolecular cyclization which causes its inactivation, and its solubility in water decreases (Jodeh et al., 2015). Dissimilarly, for SA and FP, preliminary adsorption experiments with solutions at different pHs showed that acidic conditions (pH = 2) led to removal performances of at least twice higher than at neutral pH; therefore, kinetic and equilibrium studies were conducted at acidic pH.

Kinetic studies are presented in Fig. 3a–c. They illustrate typical kinetic curves with an initial rapid increase within the first 8 h, and then reaching equilibrium within 24 h. This is consistent with availability of vacant surface sites for adsorption during initial stages and enhanced difficulty to occupy them after a lapse of time, likely because of the repulsive forces between solid molecules in bulk and solid phases (Bansal and Goyal, 2001). A pseudo-second-order rate model (Ho, 2006) was applied to describe the adsorption kinetics:

$$q_t = \frac{q_{eH}^2 k_H t}{1 + q_{eH} k_H t} \quad (1)$$

where q_t is the amount of drug adsorbed at any time t per unit mass of adsorbent [mmol/g], k_H, the rate constant of adsorption [g/mmol min], and q_{eH}, the amount of drug adsorbed at equilibrium per unit mass of adsorbent [mmol/g]. This model correlates well with kinetic data when chemisorption involving valence forces through the sharing or exchange of electrons between the adsorbate and the adsorbent constitutes the rate-limiting step. Models predictions are also displayed in Fig. 3a–c and estimated model parameters are summarized in Table 3. They were estimated by nonlinear regression analysis for a 5% significant level by minimizing the sum of the squared differences between the observed and predicted values of the dependent variable. The model enabled to describe properly most of the experimental kinetic curves, especially for SA and FP adsorption. This result is in agreement with those reported in the literature dealing with adsorption of organic solutes onto carbonaceous adsorbents (Bansal and Goyal, 2001; Fernandez et al., 2014). For the removal of DFS, a less adequate fitting of the model was obtained for HC-C and AHC-N; even so, high values of

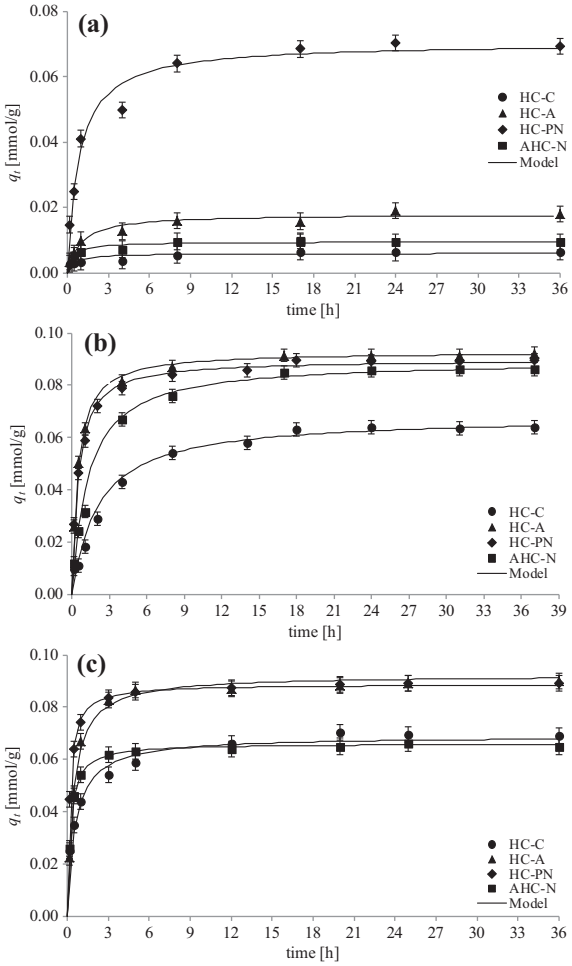

Fig. 3. Kinetic data for adsorption of (a) diclofenac sodium, (b) salicylic acid and (c) flurbiprofen onto the developed activated hydrochars. Dose: 0.5 g/L. Solutions of C_0 = 0.05 mM at pH = 2 (for salicylic acid and flurbiprofen) and pH = 7 (for diclofenac sodium). Comparison between the experimental data (points) and predictions of the pseudo-second order rate model (lines).

k_H (Table 3) estimated for these samples were outstanding, in comparison to the other activated hydrochars. The low removal of DFS obtained with these samples (also deduced from estimated q_{eH}), and in consequence their quick saturation, could explain these results. Adsorption of SA was faster onto the adsorbents that presented greater porosity development. For this drug, values of q_{eH} were more similar among the adsorbents; its smaller size (0.6 nm) (Mizaee and Hadadiyan, 2012) may have allowed the molecule to access porosity that remained unreached for the other adsorbates. Adsorption of FP was also enhanced for the samples with higher porosity. However, no clear tendency regarding the rate of adsorption was found for this drug.

The adsorption isotherms for the three drugs onto the activated hydrochars are presented in Fig. 4a–c. Two common adsorption models were comparatively applied for experimental data fitting. The Langmuir model, described by the following equation:

$$q_e = \frac{k_L q_{mL} C_e}{1 + k_L C_e} \quad (2)$$

where q_e is the amount of the drug adsorbed at equilibrium per unit mass of adsorbent [mmol/g], k_L, the Langmuir constant [L/mmol], q_{mL}, the maximum amount of adsorption corresponding to complete monolayer surface coverage [mmol/g] and C_e, the equilibrium

Table 3
Estimated parameters of the pseudo-second order kinetic model, the Langmuir and the Freundlich models for the adsorption of diclofenac sodium (DFS), salicylic acid (SA) and flurbiprofen (FP).

Kinetic model parameters	HC-C	HC-A	HC-PN	AHC-N	Drug
q_{eH} [mmol/g]	0.006	0.018	0.070	0.009	DFS
k_H [g/mmol h]	324.5	57.5	16.6	604.0	
r^2	0.721	0.953	0.971	0.905	
q_{eH} [mmol/g]	0.068	0.093	0.090	0.090	SA
k_H [g/mmol h]	7.0	24.3	23.6	8.8	
r^2	0.987	0.998	0.993	0.990	
q_{eH} [mmol/g]	0.069	0.092	0.089	0.066	FP
k_H [g/mmol h]	25.0	24.3	62.7	67.0	
r^2	0.936	0.991	0.995	0.995	
Langmuir parameters					
q_{mL} [mmol/g]	0.018	0.164	0.211	0.031	DFS
k_L [L/mmol]	4.2	2.2	27.5	13.5	
r^2	0.961	0.928	0.981	0.956	
q_{mL} [mmol/g]	0.09	0.56	0.66	0.16	SA
k_L [L/mmol]	60.9	22.0	10.9	108.3	
r^2	0.974	0.986	0.978	0.959	
q_{mL} [mmol/g]	0.83	0.65	0.61	0.64	FP
k_L [L/mmol]	6.1	85.0	83.9	15.5	
r^2	0.990	0.989	0.981	0.994	
Freundlich parameters					
n_F	0.35	0.42	0.20	0.22	DFS
k_F [(mmol/g)(L/mmol)^{n_F}]	0.013	0.106	0.203	0.027	
r^2	0.993	0.975	0.971	0.942	
n_F	0.16	0.23	0.28	0.13	SA
k_F [(mmol/g)(L/mmol)^{n_F}]	0.10	0.54	0.63	0.15	
r^2	0.954	0.947	0.941	0.990	
n_F	0.76	0.37	0.37	0.63	FP
k_F [(mmol/g)(L/mmol)^{n_F}]	1.84	1.57	1.45	1.79	
r^2	0.993	0.994	0.985	0.983	

concentration of the adsorbates in solution [mmol/L]. Also, the Freundlich model was applied, represented by:

$$q_e = k_F C_e^{n_F} \quad (3)$$

where k_F [(mol/g)(L/mmol)^{n_F}] and n_F are the Freundlich constants related to adsorption capacity and intensity, respectively. Models predictions are also displayed in Fig. 4a–c and estimated parameters obtained from these models are listed in Table 3. Adsorption isotherms for DFS obtained for the thermally activated hydrochars were better described by the Freundlich model; nevertheless, low n_F values obtained for the other samples also suggested heterogeneity of adsorption affinity. Estimated adsorption capacities for DFS obtained with HC-A and HC-PN were, respectively, two and three times higher than those reported for another biomass based AC (Jodeh et al., 2015) however lower than a commercial AC (Sotelo et al., 2012). HC-PN had the best performance in removing this drug likely because of the higher BET area (618 m^2/g) and mesopore volume (~0.1 cm^3/g) of this sample, allowing the aromatic molecule to have an easier access to the adsorption sites. Given that, except for HC-C, the rest of the adsorbents had lower p_{zc} values than the solution pH selected (pH = 7), only HC-C could have been positively charged at that pH. As a consequence, electrostatic repulsions could take place with air and acid activated hydrochars, leading to lower removal levels. However, this effect was not evident here. HC-C presented the lowest adsorption performance, probably due to steric hindrance, suggesting that the adsorption of DFS may be more related to textural properties and dispersion interactions between the drug molecule and the aromatic structure of the activated hydrochars. According to Sotelo et al. (2012), the binding of DFS would involve parallel adsorption of the drug molecule onto the carbon surface and also non-electrostatic interactions, including hydrogen bonding, might also take part.

The experimental isotherms for the adsorption of SA and FP onto the activated hydrochars, as well as the models predictions are illustrated in Fig. 4b and c, respectively. Although Langmuir model predicted more accurately the experimental isotherms for SA, similar adsorption capacities (q_{mL} and k_F) were estimated by both models. Again, HC-A and HC-PN showed the best performances and their capacities were similar to that reported by Rakić et al. (2015) for commercial ACs. As observed, the acidic pH enhanced the uptake of both SA (pKa = 2.98) and FP (pKa = 4.24) (Ayranci and Duman, 2006; Osmani et al., 2012). With solutions at pH 2, namely below the activated hydrochars' p_{zc}, the adsorption performance of the adsorbents increased significantly in comparison to that reported for DFS. At that pH, all the activated hydrochars might be positively charged and both SA and FP are expected mainly in their neutral forms. Hence, the dispersion interactions and, to a certain extent, the electrostatic interactions between the positively charged surface and either the π electrons of the aromatic ring or the dipole of the adsorbates may have been responsible for the higher adsorption obtained (Ayranci and Duman, 2006). Estimated adsorption capacities for FP were comparatively high, even for the activated hydrochars which did not perform very well as adsorbents for DFS and SA. The low solubility of FP may be responsible for these experimental curves which seemed restricted to low equilibrium concentrations. Akçay et al. (2009) reported adsorption of FP onto montmorillonite and differ-

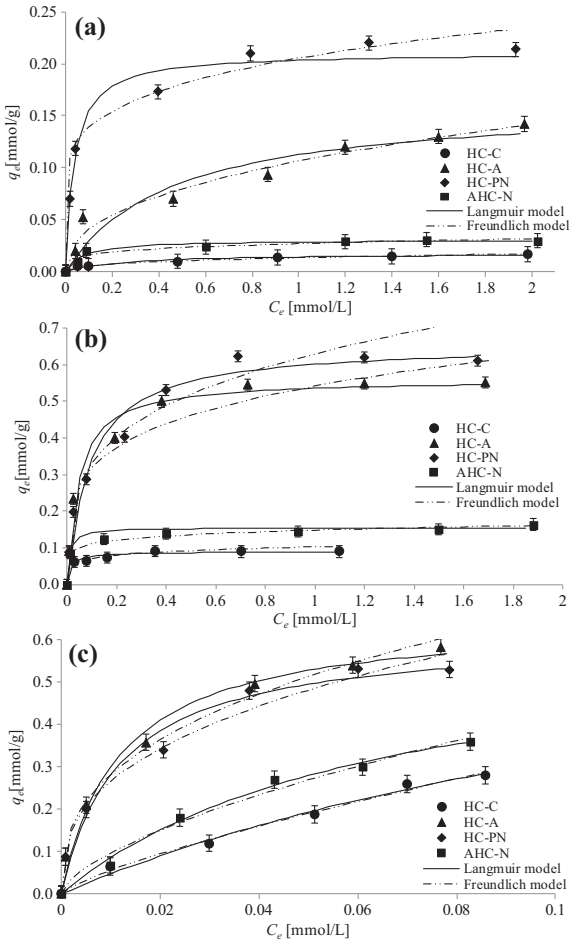

Fig. 4. Equilibrium isotherms for adsorption of (a) diclofenac sodium, (b) salicylic acid and (c) flurbiprofen onto the developed activated hydrochars. Comparison between the experimental data (points) and predictions of Langmuir and Freundlich models (lines). Solutions at pH = 2 (for salicylic acid and flurbiprofen) and pH = 7 (for diclofenac sodium).

ences of one order of magnitude for adsorption capacities were estimated using different models, therefore it is difficult to compare with those obtained here. It should also be highlighted that adsorption of FP has not been previously reported using carbonaceous adsorbents.

4. Conclusions

Hydrothermal carbonization of orange peels provided a carbonaceous solid product that was successfully used as precursor to obtain good adsorbents for emerging pharmaceutical contaminants, applying thermal and chemical activation processes. The activation conditions deeply affected the morphology and surface functionalities of the materials obtained. In general, textural characteristics of the adsorbents and the solutions pH had the biggest impact on the adsorption performance for the investigated drugs. HC-PN and HC-A, with higher development of porosity, showed the best adsorption behavior as adsorbents and further tuning of these materials may open the spectrum of applications.

Acknowledgements

M.E.F., P.R.B. and A.L.C. gratefully acknowledge Consejo Nacional de Investigaciones Científicas y Técnicas (CONICET), Universidad de Buenos Aires and Agencia Nacional de Promoción Científica y Tecnológica (ANPCyT-FONCyT) from Argentina, for their financial support. S.R. and B.L. gratefully acknowledge Gobierno de Extremadura for support from Project GRU10159. Besides, M.E.F. is grateful to Asociación Universitaria Iberoamericana de Posgrado (AUIP) from Spain for the mobility grant and CONICET for its support.

Appendix A. Supplementary data

Supplementary data associated with this article can be found, in the online version, at http://dx.doi.org/10.1016/j.biortech.2015.02.035.

References

Akçay, G., Kılınç, E., Akçay, M., 2009. The equilibrium and kinetics studies of flurbiprofen adsorption onto tetrabutylammonium montmorillonite (TBAM). Colloids Surf., A 335 (1–3), 189–193.
Ayranci, E., Duman, O., 2006. Adsorption of aromatic organic acids onto high area activated carbon cloth in relation to wastewater purification. J. Hazard. Mater. B136, 542–552.
Bansal, R.C., Goyal, M., 2001. Activated Carbon Adsorption. Ed. Taylor & Francis, London.
Carrott, P.J.M., Nabais, J.M.V., Ribeiro Carrott, M.M.L., Menéndez, J.A., 2001. Thermal treatments of activated carbon fibers using a microwave furnace. Microporous Mesoporous Mater. 47, 243–252.
Chen, B., Chen, Z., 2009. Sorption of naphthalene and 1-naphthol by biochars of orange peels with different pyrolytic temperatures. Chemosphere 76, 127–133.
Delgado, L.F., Charles, P., Glucina, K., Morlay, C., 2012. The removal of endocrine disrupting compounds, pharmaceutically activated compounds and cyanobacterial toxins during drinking water preparation using activated carbon – A review. Sci. Total Environ. 435, 509–525.
Falco, C., Marco-Lozar, J.P., Salinas-Torres, D., Morallón, E., Cazorla-Amorós, D., Titirici, M.M., Lozano-Castelló, D., 2013. Tailoring the porosity of chemically activated hydrothermal carbons: influence of the precursor and hydrothermal carbonization temperature. Carbon 62, 346–355.
FAS-USDA (Foreign Agricultural Service-United States Department of Agriculture). Citrus: world markets and trade, 2014. Consulted on 20th February 2014. Available from: <http://apps.fas.usda.gov/psdonline/circulars/citrus.pdf>.
Fernandez, M.E., Nunell, G.V., Bonelli, P.R., Cukierman, A.L., 2014. Activated carbon developed from orange peels: batch and dynamic competitive adsorption of basic dyes. Ind. Crops Prod. 62, 437–445.
Funke, A., Ziegler, F., 2010. Hydrothermal carbonization of biomass: a summary and discussion of chemical mechanisms for process engineering. Biofuels, Bioprod. Biorefin. 4, 160–177.
Gañán, J., González, J.F., González-García, C.M., Ramiro, A., Sabio, E., Román, S., 2006. Air-activated carbons from almond tree pruning: preparation and characterization. Appl. Surf. Sci. 252, 5988–5992.
Hao, W., Björkman, E., Lilliesträle, M., Hedin, N., 2013. Activated carbons prepared from hydrothermally carbonized waste biomass used as adsorbents for CO_2. Appl. Energy 12, 526–532.
Ho, Y.S., 2006. Review of second-order models for adsorption systems. J. Hazard. Mater. 136, 681–689.
Jagtoyen, M., Derbyshire, F., 1998. Activated carbons from yellow poplar and white oak by H_3PO_4 activation. Carbon 36 (7–8), 1085–1097.
Jodeh, S., Abdelwahab, F., Jaradat, N., Warad, I., Jodehc, W., 2015. Adsorption of diclofenac from aqueous solution using *Cyclamen persicum* tubers based activated carbon (CTAC). J. Assoc. Arab Univ. Basic Appl. Sci. (In press)
Li, M., Li, W., Liu, S., 2011. Hydrothermal synthesis, characterization, and KOH activation of carbon spheres from glucose. Carbohydr. Res. 346, 999–1004.
Lu, X., Flora, J.R.V., Berge, N.D., 2014. Influence of process water quality on hydrothermal carbonization of cellulose. Bioresour. Technol. 154, 229–239.
Luo, Y., Guo, W., Ngo, H.H., Nghiem, L.D., Hai, F.I., Zhang, J., Liang, S., Wang, X.C., 2014. A review on the occurrence of micropollutants in the aquatic environment and their fate and removal during wastewater treatment. Sci. Total Environ. 473–474, 619–641.
Lynam, J.G., Coronella, C.J., Yan, W., Reza, M.T., Vasquez, V.R., 2011. Acetic acid and lithium chloride effects on hydrothermal carbonization of lignocellulosic biomass. Bioresour. Technol. 102, 6192–6199.
Mizaee, F., Hadadiyan, E., 2012. Approximate solutions for mixed nonlinear Volterra–Fredholm type integral equations via modified Block Pulse functions. J. Assoc. Arab. Univ. Basic Appl. Sci. 12, 65–73.
Oliveira, I., Blöhse, D., Ramke, H.G., 2013. Hydrothermal carbonization of agricultural residues. Bioresour. Technol. 142, 138–146.
Osmani, O., Hughes, H., McLoughlin, P., 2012. Probing the recognition of molecularly imprinted polymer beads. J. Mater. Sci. 47, 2218–2227.
Parshetti, G.K., Hoekman, S.K., Balasubramanian, R., 2013. Chemical, structural and combustion characteristics of carbonaceous products obtained by hydrothermal carbonization of palm empty fruit bunches. Bioresour. Technol. 135, 683–689.
Rakić, V., Rac, V., Kmar, M., Otman, O., Auroux, A., 2015. The adsorption of pharmaceutically active compounds from aqueous solutions onto activated carbons. J. Hazard. Mater. 282, 141–149.
Rodriguez Reinoso, F., 2002. Production and applications of activated carbons. In: Schüth, F., Sing, K.S.W., Weitkamp, J. (Eds.), Handbook of Porous Solids. Wiley/VCH, pp. 1766–1827.
Román, S., Nabais, J.M.V., Laginhas, C., Ledesma, B., González, J.F., 2012. Hydrothermal carbonization as an effective way of densifying the energy content of biomass. Fuel Process. Technol. 103, 78–83.
Román, S., Valente Nabais, J.M., Ledesma, B., González, J.F., Laginhas, C., Titirici, M.M., 2013. Production of low-cost adsorbents with tunable surface chemistry by conjunction of hydrothermal carbonization and activation processes. Microporous Mesoporous Mater. 165, 127–133.
Schiewer, S., Iqbal, M., 2010. The role of pectin in Cd binding by orange peel biosorbents: a comparison of peels, depectinated peels and pectic acid. J. Hazard. Mater. 177, 899–907.
Sevilla, M., Maciá-Agulló, J.A., Fuertes, A.B., 2011. Hydrothermal carbonization of biomass as a route for the sequestration of CO_2: chemical and structural properties of the carbonized products. Biomass Bioenergy 35, 3152–3159.
Sotelo, J.L., Rodríguez, A., Álvarez, S., García, J., 2012. Removal of caffeine and diclofenac on activated carbon in fixed bed column. Chem. Eng. Res. Des. 90, 967–974.
Thirumavalavan, M., Lai, Y.L., Lee, J.F., 2011. Fourier transform infrared spectroscopic analysis of fruit peels before and after the adsorption of heavy metal ions from aqueous solution. J. Chem. Eng. Data 56, 2249–2255.
Titirici, M.M., Thomas, A., Yu, S.H., Müller, J.O., Antonietti, M., 2007. A direct synthesis of mesoporous carbons with bicontinuous pore morphology from crude plant material by hydrothermal carbonization. Chem. Mater. 19, 4205–4212.
Verlicchi, P., Al Aukidy, M., Zambello, E., 2012. Occurrence of pharmaceutical compounds in urban wastewater: removal, mass load and environmental risk after a secondary treatment – A review. Sci. Total Environ. 429, 123–155.
Vernersson, T., Bonelli, P.R., Cerrella, E.G., Cukierman, A.L., 2002. *Arundo donax* cane as a precursor for activated carbons preparation by phosphoric acid activation. Bioresour. Technol. 83, 95–104.
White, R.J., Budarin, V.L., Clark, J.H., 2010. Pectin-derived porous materials. Chem. Eur. J. 16, 1326–1335.